



Differentiating focal autoimmune pancreatitis and pancreatic ductal adenocarcinoma: contrast-enhanced MRI with special emphasis on the arterial phase

Ji Hye Kwon¹ · Jin Hee Kim¹ · So Yeon Kim¹ · Jae Ho Byun¹ · Hyoung Jung Kim¹ · Moon-Gyu Lee¹ · Seung Soo Lee¹

Received: 20 December 2018 / Revised: 21 March 2019 / Accepted: 25 March 2019 / Published online: 26 April 2019
© European Society of Radiology 2019

Abstract

Objectives To compare focal-type autoimmune pancreatitis (AIP) and pancreatic ductal adenocarcinoma (PDA) using contrast-enhanced MR imaging (CE-MRI), and to assess diagnostic performance of the lesion contrast at arterial phase (AP) ($\text{Contrast}_{\text{AP}}$) for differentiating between the two diseases.

Methods Thirty-six patients with focal-type AIP and 72 patients with PDA were included. All included patients underwent CE-MRI with triple phases. The signal intensity (SI) of the mass and normal pancreas was measured at each phase, and the lesion contrast ($\text{SI}_{\text{pancreas}}/\text{SI}_{\text{mass}}$) was compared between AIP and PDA groups. The sensitivity and specificity of $\text{Contrast}_{\text{AP}}$ using an optimal cutoff point were compared with those of key imaging features specific to AIP and PDA.

Results The lesion contrast differed significantly between AIP and PDA groups at all phases of CE-MRI; the maximum difference was observed at AP. For AIP, the sensitivity (94.4%) and specificity (87.5%) of $\text{Contrast}_{\text{AP}}$ (cutoff ≤ 1.41) were comparable or significantly higher than those of all key imaging features (sensitivity, 38.9–88.9%; specificity, 48.6–95.8%), except for the halo sign. For PDA, the sensitivity (87.5%) and specificity (94.4%) of $\text{Contrast}_{\text{AP}}$ (cutoff > 1.41) were comparable or significantly higher than those of all key imaging features (sensitivity, 40.3–68.1%; specificity, 72.2–94.4%), except for the discrete mass.

Conclusions Quantitative analysis of the lesion contrast using CE-MRI, particularly at AP, was helpful to differentiate focal-type AIP from PDA. The diagnostic performance of $\text{Contrast}_{\text{AP}}$ was mostly comparable or higher than those of the key imaging features.

Key Points

- *Diagnosis of focal-type AIP vs. PDA using imaging techniques is extremely challenging.*
- *Lesion contrast in the arterial-phase MRI differs significantly between focal-type AIP and PDA.*
- *Quantitative analysis of lesion contrast using CE-MRI, particularly at the arterial phase, is helpful to differentiate focal-type AIP from PDA.*

Keywords Pancreatic neoplasms · Pancreatitis · Autoimmune disease · Carcinoma, pancreatic ductal · Magnetic resonance imaging

Abbreviations

AIP Autoimmune pancreatitis
AP Arterial phase

AUROC Area under receiver operating characteristic curve
CE-MRI Contrast-enhanced magnetic resonance imaging
DP Delayed phase
MPD Main pancreatic duct
PDA Pancreatic ductal adenocarcinoma
PP Portal phase
ROC Receiver operating characteristic
ROI Region of interest
SI Signal intensity
UP Unenhanced phase

✉ Jin Hee Kim
kimjhrad@amc.seoul.kr

¹ Department of Radiology and Research Institute of Radiology, University of Ulsan College of Medicine, Asan Medical Center, 88 Olympic-ro 43-gil, Songpa-Gu, Seoul 05505, South Korea

Introduction

Autoimmune pancreatitis (AIP) is a rare but distinctive type of chronic pancreatitis, which responds dramatically well to steroid therapy [1]. AIP can mimic pancreatic ductal adenocarcinoma (PDA), and characterization is important to avoid unnecessary surgery in patients with AIP [2–5]. Non-diffuse-type (i.e., focal and multifocal-type) AIP is challenging while diffuse-type AIP commonly manifests as a characteristic “sausage-like” pancreatic swelling, very different from PDA [2–4]. In multifocal-type AIP, magnetic resonance imaging (MRI) clearly demonstrates multiple pancreatic masses and multiple pancreatic duct strictures, highly specific for AIP [6]. Conversely, focal-type AIP, representing 28–48% of all AIP [7–10], is very difficult to differentiate from PDA as both diseases manifest as a single focal pancreatic mass and pancreatic duct stricture.

Attempts to differentiate focal-type AIP and PDA have been reported using computed tomography (CT) or MRI [11–18]. Some key differentiating features with regard to morphology of the pancreatic mass and pattern of the pancreatic duct stricture were identified. Several studies assessed the dynamic enhancement pattern of focal-type AIP using contrast-enhanced MRI (CE-MRI) mostly focused on the delayed enhancement [11–14]. The enhancement pattern at the arterial phase (AP) received little attention. Few studies have described merely “hypointensity” of focal-type AIP at the AP [11–13]. However, we observed in daily practice a clear difference in enhancement pattern or lesion contrast at the AP between focal-type AIP and PDA. Therefore, we initiated this study to compare quantitatively the lesion contrast between focal-type AIP and PDA using CE-MRI with an emphasis on the AP, and we assessed the diagnostic performance of the lesion contrast at the AP for differentiating between the two diseases.

Materials and methods

Study population

This retrospective study was approved by our institutional review board; patient informed consent was waived. In our institution’s medical database, we identified 169 patients diagnosed with AIP according to the Asian criteria [19], HISORt criteria [20], or international consensus diagnostic criteria [21] between January 2007 and December 2016 (Fig. 1). Among these, we finally included 36 patients (21 men, 15 women; mean age \pm standard deviation, 56.7 \pm 11.6 years (range, 18–75 years)) based on the following inclusion criteria: (a) the presence of CE-MRI, including unenhanced (UP), arterial (AP), portal (PP), and delayed (DP) phases before steroid treatment; (b) focal-type AIP; (c)

the absence of obvious extrapancreatic organ involvement, including sclerosing cholangitis, renal involvement, and retroperitoneal fibrosis, potentially affecting blinded image interpretation; and (d) the presence of normal pancreatic parenchyma with normal-appearing signal intensity (SI) on T1-weighted images, which was localized downstream to the mass, and was thus available for quantitative analysis. In criterion (b), the focal type was defined as the presence of a single focal mass involving less than half of the total pancreas on MRI. Cases with a mass involving $> 50\%$ pancreas (i.e., diffuse type) or multiple masses involving ≥ 2 sites (i.e., multifocal type) were excluded. Among the 36 finally included patients with focal-type AIP, 16, 5, and 15 had lesions in the head, body, and tail, respectively.

From January 2013 to December 2015, 782 patients underwent curative-intent surgery for PDA in our institution (Fig. 1). To create a 1:2 matching with the AIP group, we randomly selected 72 (49 men, 23 women; 60.5 \pm 9.6 years (40–78 years)) among the 660 patients with PDA who underwent CE-MRI before surgery, using a random number generator (QuickCalcs, GraphPad Software). The presence of normal pancreatic parenchyma downstream to the mass was also considered as stated in criterion (d) of AIP. Of the 72 patients, 47, 15, and 10 had lesions in the head, body, and tail, respectively.

MRI techniques

The MRI examinations were performed using a 1.5-T unit (Magnetom Avanto; Siemens Healthineers). Transverse T2-weighted images, MR cholangiopancreatography, and transverse T1-weighted images (CE-MRI) were obtained (Table 1). The CE-MRI was obtained using three-dimensional spoiled gradient-echo sequence, including UP and dynamic triple phases at 10 s (AP), 50 s (PP), and 3 min (DP) after intravenously injecting gadoteric acid (Dotarem; Guerbet; 0.2 mmol/kg body weight) at 2 mL/s, followed by a 20-mL saline flush, using an autoinjector. Secretin was not used in any patient.

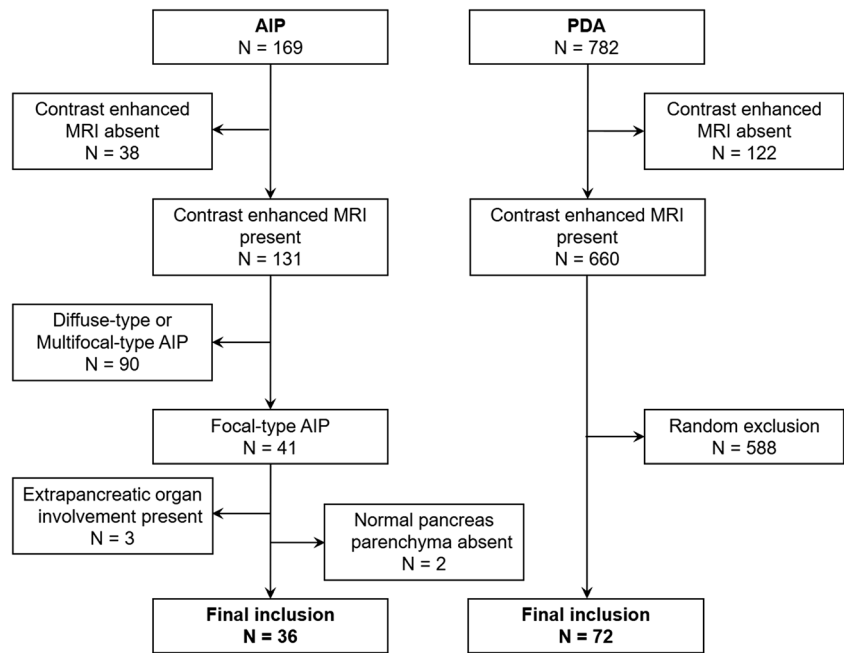
Image analysis

All images were reviewed using a local picture archiving and communication system monitor and digital imaging and communications in medicine imaging software. The patient order was randomized to avoid any patterns in the sequence of patient categories. The reviewers were blinded to the clinical data, imaging results, and final diagnosis but knew that the study population consisted of AIP and PDA.

Lesion contrast

For quantitative analysis of the lesion contrast in AIP and PDA, a board-certified abdominal radiologist performed the

Fig. 1 Flow diagram showing the selection of the study population



region-of-interest (ROI) measurement to assess the SI of the pancreatic mass and normal pancreatic parenchyma on CE-MRI. For the pancreatic mass, a round ROI was carefully placed to encompass the maximum mass area on the image wherein the mass was the most clearly visualized (Fig. 2). The peripheral enhancing portion of the mass, if present, was also included in the ROI. For the normal pancreatic parenchyma, the largest possible round ROI was carefully placed in a homogeneous region of the pancreas excluding any recognizable vessels or other non-parenchymal structures; this was performed in a downstream location to the mass to exclude any potential obstructive pancreatitis-related SI change (Fig. 2). The SI of the pancreatic mass and the normal pancreatic parenchyma was measured three times for the same image for each phase; average SI values were calculated to obtain the lesion contrast at each phase using the following equation: $\text{Contrast} = \text{SI}_{\text{pancreas}} / \text{SI}_{\text{mass}}$.

For qualitative analysis of the lesion contrast, two radiologists visually assessed the CE-MRI to determine in consensus the best phase showing the largest SI difference between the mass and the normal pancreas. They also visually evaluated whether the lesion contrast changed from UP to AP (decreased, unchanged, or increased).

Key imaging features

Two radiologists reviewed all MRI examinations of the patients to determine in consensus the presence of the following key imaging features for differentiating between focal-type AIP and PDA [11–18, 22, 23]: discrete pancreatic mass (discernible focal hypointense mass with visible border between the mass and the normal pancreas) on UP and on dynamic

triple phases, separately; speckled appearance (speckled hyperintense areas relative to that of the surrounding lesion on UP or AP) [15, 17]; target enhancement (layered pattern enhancement, typically a hypoenhancing lesion surrounded by hyperenhancement); delayed enhancement (hypoenhancement on AP and iso- or hyperenhancement on PP or DP compared to the normal pancreas) and pattern (homogeneous vs. heterogeneous) of the mass; halo sign (thin or thick, continuous, rim-like hypoenhancing soft tissue lesion outlining the pancreas); main pancreatic duct (MPD) stricture and its pattern (abrupt vs. tapered narrowing); duct penetrating sign (visible MPD penetrating the mass without being completely obstructed by the mass); upstream MPD dilatation (absent, mild (< 5 mm) or marked (≥ 5 mm)); and upstream pancreatic atrophy.

Statistical analysis

The lesion contrast obtained by ROI measurement at each phase of CE-MRI was compared between AIP and PDA groups using the Student *t* test. For the lesion contrast at each phase, the receiver operating characteristic (ROC) analysis was performed to compare the area under the ROC curve (AUROC) for distinguishing AIP from PDA among the phases. For the phase with the largest AUROC, the optimal cutoff point of the lesion contrast to maximize both the sensitivity and specificity on ROC curve (i.e., Youden index) was determined. The sensitivity and specificity of the lesion contrast at the phase when using the optimal cutoff point were compared with those of the key imaging features for the diagnosis of AIP and PDA using McNemar's test. The frequencies of categorical variables for the qualitative analysis of the visually assessed lesion contrast and the key imaging features

Table 1 MRI sequences and parameters

| | T2-weighted images | | MRCP | CE-MRI |
|----------------------|--------------------|--------------|------------------|-----------------|
| | HASTE | RT-TSE | Single-shot RARE | VIBE |
| TR/TE (ms) | Infinite/154 | 3600–5100/96 | Infinite/1000 | 4.1–4.2/1.5–1.7 |
| Flip angle (°) | 150 | 150 | 180 | 10 |
| Field of view (mm) | 240 × 350 | 240 × 350 | 300 × 300 | 280 × 350 |
| Matrix | 192 × 256 | 264 × 384 | 320 × 320 | 256 × 320 |
| Slice thickness (mm) | 6 | 6 | 40 | 4 |
| Interslice gap (mm) | 1.2 | 1.2 | 0 | 0 |
| Echo train length | 256 | 13 | 256 | NA |

For all sequences, fat saturation was employed using the chemical shift-selective fat suppression technique

Abbreviations: MRCP, magnetic resonance cholangiopancreatography; CE-MRI, contrast-enhanced magnetic resonance imaging; HASTE, half-Fourier acquisition single-shot turbo spin-echo; RT-TSE, respiratory-triggered turbo spin-echo; RARE, rapid acquisition with relaxation enhancement; VIBE, volumetric interpolated breath-hold examination; TR, repetition time; TE, echo time; NA, not applicable

were compared between AIP and PDA groups using chi-square test or Fisher's exact test, as appropriate. $P < 0.05$ was considered statistically significant. SPSS for Windows version 21.0 (IBM Corp.) and MedCalc for Windows version 12.5.0.0 (MedCalc) were used for the statistical analyses.

Results

Lesion contrast: AIP vs. PDA

The quantitative analysis results regarding the lesion contrast are summarized in Table 2. The lesion contrast differed significantly between AIP and PDA groups at all phases of CE-

MRI ($p \leq 0.008$). The lesion contrast in AIP was the highest at UP, whereas in PDA, it was the highest at AP. The dynamic pattern of the lesion contrast remarkably differed between the two groups (Fig. 3). In AIP, the lesion contrast, which was the highest at UP, gradually decreased as the phase passed. The contrast ultimately declined to less than 1.0 at DP (33 of 36, 91.7%), indicating reversal of SI between the mass and normal parenchyma. In PDA, the lesion contrast increased from UP to AP and progressively decreased thereafter. The contrast remained 1.0 or higher in most lesions (58 of 72, 80.6%) at DP in contrast with AIP. The maximum difference of the lesion contrast between AIP and PDA was observed at AP.

Table 3 shows the qualitative analysis results regarding the visually assessed lesion contrast. In AIP, the largest SI

Fig. 2 Examples of ROI measurement in patients with AIP (a, b) and PDA (c, d). Unenhanced-phase T1-weighted MR images show ROIs placed in the pancreatic masses (a, c) and normal pancreatic parenchymas (b, d), which are localized downstream to the mass

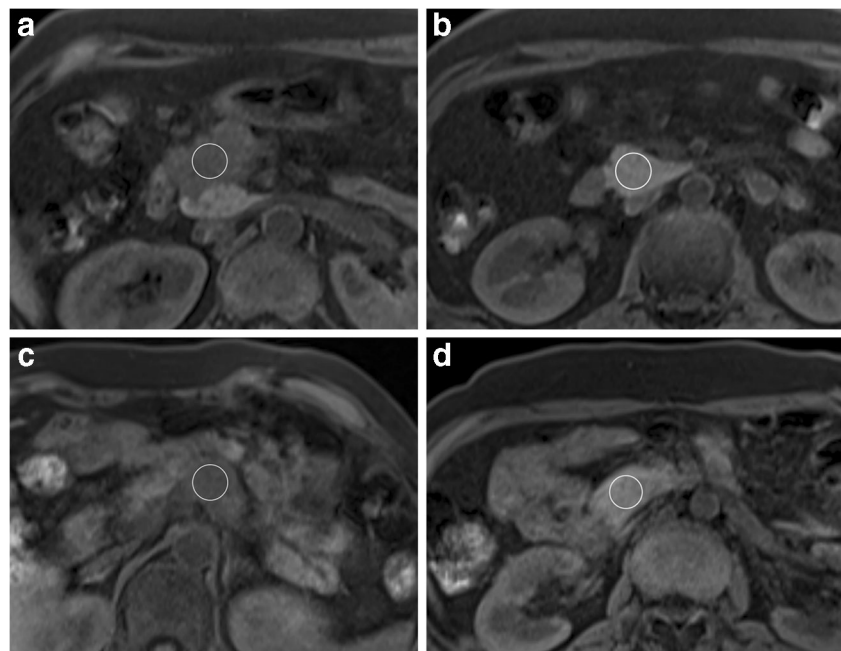


Table 2 Quantitative analysis of the lesion contrast by ROI measurement

| | AIP (<i>n</i> = 36) | PDA (<i>n</i> = 72) | <i>p</i> value | AUROC [#] | <i>p</i> value* |
|---|------------------------|------------------------|----------------|---------------------|-----------------|
| Contrast _{UP} , mean [range, SD] | 1.49 [1.15–2.03, 0.21] | 1.60 [1.23–2.06, 0.19] | 0.008 | 0.651 [0.553–0.740] | < 0.001 |
| Contrast _{AP} , mean [range, SD] | 1.23 [0.95–1.73, 0.16] | 1.84 [1.25–3.16, 0.38] | < 0.001 | 0.957 [0.900–0.987] | |
| Contrast _{PP} , mean [range, SD] | 1.00 [0.79–1.28, 0.13] | 1.44 [0.98–2.11, 0.28] | < 0.001 | 0.940 [0.877–0.976] | 0.407 |
| Contrast _{DP} , mean [range, SD] | 0.88 [0.71–1.15, 0.10] | 1.21 [0.76–1.84, 0.25] | < 0.001 | 0.910 [0.839–0.956] | 0.111 |

Abbreviations: UP, unenhanced phase; AP, arterial phase; PP, portal phase; DP, delayed phase

[#] Area under receiver operating characteristic curve for differentiating between AIP and PDA (95% confidence interval)

*Compared with AUROC of Contrast_{AP}

difference between the mass and the normal pancreas was observed the most frequently at UP (66.7%), followed by DP and AP. Conversely, in PDA, this maximum difference was most frequently observed at AP (69.4%). Between UP and AP, the lesion contrast decreased in 26/36 (72.2%) AIP patients, whereas it increased in 56/72 (77.8%) PDA patients. In 10 (27.8%) AIP and eight (11.1%) PDA patients, there were no perceivable contrast changes between UP and AP.

Key imaging features: AIP vs. PDA

Table 4 shows the comparative results of the key imaging features for AIP and PDA. The speckled appearance, delayed homogeneous enhancement, halo sign, MPD tapered narrowing, and duct penetrating sign were significantly more prevalent in AIP than in PDA (*p* < 0.001). The discrete mass on AP/PP/DP, target enhancement, MPD abrupt narrowing,

upstream MPD marked dilatation, and upstream pancreatic atrophy were significantly more prevalent in PDA than in AIP (*p* < 0.001). The discrete mass on UP was more prevalent in PDA than in AIP; however, the difference was not statistically significant (*p* = 0.084). Representative cases are presented in Figs. 4 and 5.

Sensitivity and specificity for AIP and PDA: lesion contrast vs. key imaging features

Among all phases of CE-MRI, the AUROC of the lesion contrast for distinguishing AIP from PDA was the largest at AP (0.957) (Table 2) (Fig. 6). The optimal cutoff point of the lesion contrast at AP (Contrast_{AP}) calculated by ROC analysis was 1.41. The sensitivity and specificity of Contrast_{AP} for the diagnosis of AIP using the optimal cutoff point of 1.41 were 94.4% and 87.5%, respectively, and vice versa for PDA. Table 5 shows the comparison of these sensitivity and specificity values of Contrast_{AP} and those of the key imaging features. Overall, both the sensitivity and specificity of Contrast_{AP} were mostly comparable or even higher in comparison with those of the key imaging features. More specifically, the specificity of only halo sign, a key imaging feature

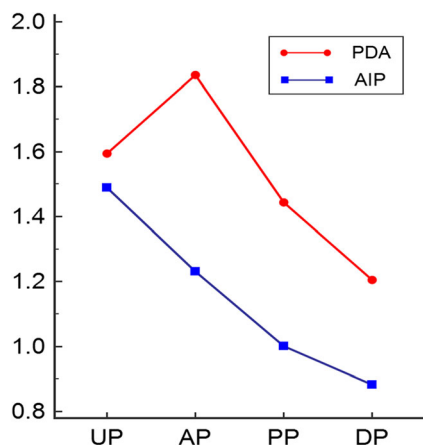


Fig. 3 Dynamic pattern of the lesion contrast in focal-type AIP and PDA. Horizontal axis and vertical axis indicate the phases of CE-MRI (UP, unenhanced phase; AP, arterial phase; PP, portal phase; and DP, delayed phase) and the mean value of the lesion contrast (SI_{pancreas}/SI_{mass}), respectively. In AIP, the lesion contrast is the highest at UP and it gradually decreases as the phase passes, being less than 1.0 (mean, 0.88) at DP. In PDA, the lesion contrast increases between UP and AP, and decreases progressively thereafter. Note that the maximum difference of the lesion contrast between AIP and PDA is observed at AP (1.23 vs. 1.84, *p* < 0.001)

Table 3 Qualitative analysis of the lesion contrast by visual assessment

| | AIP (<i>n</i> = 36) (%) | PDA (<i>n</i> = 72) (%) | <i>p</i> value |
|-------------------------|--------------------------|--------------------------|----------------|
| Best phase [#] | | | < 0.001 |
| Unenhanced phase | 24 (66.7) | 15 (20.8) | |
| Arterial phase | 5 (13.9) | 50 (69.4) | |
| Portal phase | 0 (0) | 3 (4.2) | |
| Delayed phase | 7 (19.4) | 4 (5.6) | |
| Contrast change* | | | < 0.001 |
| Decreased | 26 (72.2) | 8 (11.1) | |
| Unchanged | 10 (27.8) | 8 (11.1) | |
| Increased | 0 (0) | 56 (77.8) | |

[#] Best phase showing the largest SI difference between the mass and the normal pancreas

*Change of the lesion contrast from unenhanced phase to arterial phase

Table 4 Comparison of the key imaging features for AIP and PDA

| | AIP (<i>n</i> = 36) (%) | PDA (<i>n</i> = 72) (%) | <i>p</i> value |
|-----------------------------|--------------------------|--------------------------|----------------|
| Discrete mass on UP | 24 (66.7) | 60 (83.3) | 0.084 |
| Discrete mass on AP/PP/DP | 10 (27.8) | 69 (95.8) | < 0.001 |
| Speckled appearance | 32 (88.9) | 37 (51.4) | < 0.001 |
| Target enhancement | 2 (5.6) | 49 (68.1) | < 0.001 |
| Delayed enhancement | | | < 0.001 |
| Absent | 2 (5.6) | 24 (33.3) | |
| Homogeneous | 29 (80.6) | 4 (5.6) | |
| Heterogeneous | 5 (13.9) | 44 (61.1) | |
| Halo sign | 14 (38.9) | 0 (0) | < 0.001 |
| MPD stricture | | | < 0.001 |
| Absent | 2 (5.6) | 6 (8.3) | |
| Tapered | 31 (86.1) | 20 (27.8) | |
| Abrupt | 3 (8.3) | 46 (63.9) | |
| Duct penetrating sign | 14 (38.9) | 3 (4.2) | < 0.001 |
| Upstream MPD dilatation | | | < 0.001 |
| Absent | 18 (50) | 13 (18.1) | |
| Mild (< 5 mm) | 16 (44.4) | 30 (41.7) | |
| Marked (≥ 5 mm) | 2 (5.6) | 29 (40.3) | |
| Upstream pancreatic atrophy | 4 (11.1) | 37 (51.4) | < 0.001 |

Abbreviations: UP, unenhanced phase; AP, arterial phase; PP, portal phase; DP, delayed phase; MPD, main pancreatic duct

for AIP, was significantly higher than that of $\text{Contrast}_{\text{AP}}$. Otherwise, the specificity and sensitivity of $\text{Contrast}_{\text{AP}}$ for AIP were significantly higher than or comparable to those of the key imaging features. For PDA, the sensitivity of $\text{Contrast}_{\text{AP}}$ was significantly higher than those of all key imaging features, except for the discrete mass, and its specificity was also higher or comparable.

Discussion

Our study showed that the lesion contrast at AP was significantly lower in AIP than in PDA and quantitative analysis of the lesion contrast using CE-MRI could be helpful for distinguishing focal-type AIP from PDA. Our findings suggest that $\text{Contrast}_{\text{AP}}$ can be used as an important quantitative

Fig. 4 A 59-year-old man with focal-type AIP. The pancreatic mass (arrows) in the tail appears discrete hypointensity at the unenhanced phase (a) and ill-defined, subtle hypo- or isointensity at the arterial phase (b). The lesion contrast ($\text{SI}_{\text{pancreas}}/\text{SI}_{\text{mass}}$) remarkably decreased between unenhanced (1.75) and arterial (1.03) phase. The portal (c) and delayed (d) phase images clearly demonstrate the homogeneous hyperintensity of the mass

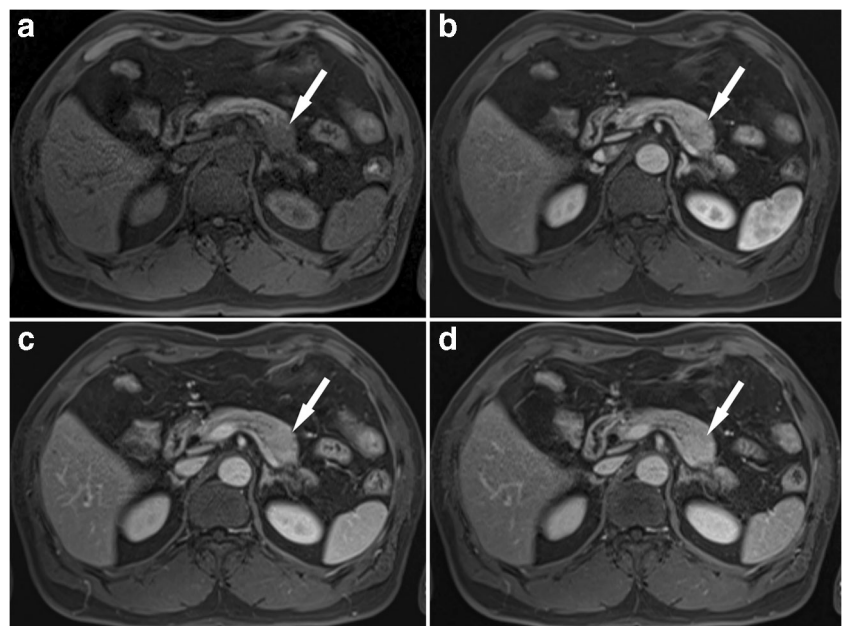
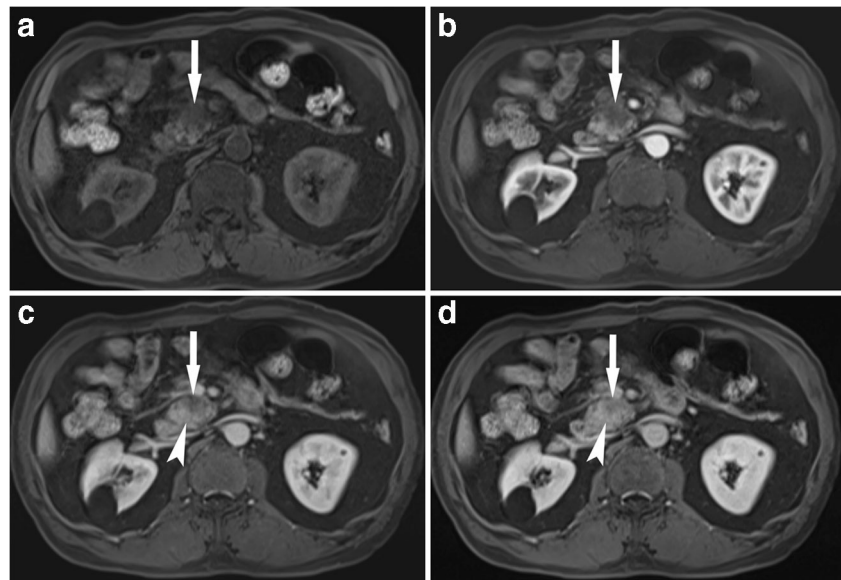


Fig. 5 A 69-year-old man with PDA. The pancreatic mass (arrows) in the head appears discrete hypointensity on both unenhanced (a) and arterial (b) phases. However, the lesion contrast ($SI_{\text{pancreas}}/SI_{\text{mass}}$) increased between unenhanced (1.73) and arterial (2.33) phases, and thus, the mass appears more conspicuous on arterial phase than on unenhanced phase. During the portal (c) and delayed (d) phases, the mass progressively enhances, and the lesion periphery (arrowheads) appears isointensity or mild hyperintensity, but the lesion center still maintains hypointensity



index for differentiating between the two diseases considering its excellent diagnostic performance when compared to those of the existing key imaging features. The sensitivity of $\text{Contrast}_{\text{AP}}$ (94.4%) for AIP (cutoff ≤ 1.41) was strikingly higher than that of the halo sign (38.9%). The halo sign is a representative imaging feature of AIP; however, its major drawback is poor sensitivity. In recent studies of more than 20 patients with focal-type AIP, the sensitivity of halo sign was very low at 14.6–47.5% [13–15]. Similarly, the duct penetrating sign also had high specificity (95.8%) but poor sensitivity (38.9%). The speckled appearance in AIP is considered to be due to the normal or less-affected pancreatic lobules within an inflammatory mass and has been reported to be specific for AIP in previous studies using CT [15] and MRI

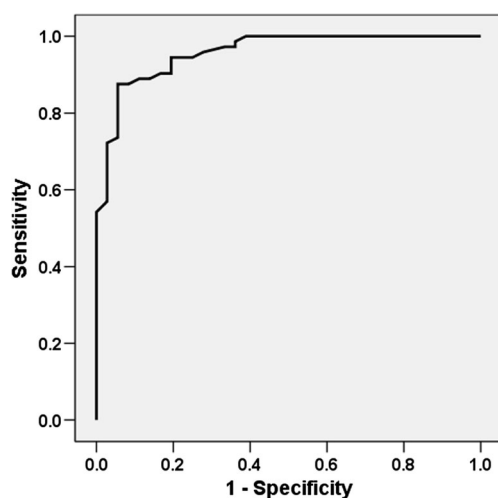


Fig. 6 ROC curve for the lesion contrast at the arterial phase ($\text{Contrast}_{\text{AP}}$). The area under the ROC curve of $\text{Contrast}_{\text{AP}}$ for distinguishing AIP from PDA was 0.957, which was the largest among the all phases of CE-MRI

[17]. However, in this study, its specificity for AIP was only 48.6%, presumably because heterogeneous enhancement of PDA may seem similar to the speckled appearance of AIP. Among the key imaging features of AIP, delayed homogeneous enhancement was the only one with high sensitivity (80.6%) and specificity (94.4%), which were comparable to that of $\text{Contrast}_{\text{AP}}$. A few previous studies comparing the enhancement patterns of focal-type or mass-forming AIP and PDA have also reported high sensitivity and specificity of delayed homogeneous enhancement [11, 16, 18], which was highlighted again in our study. Quantitative analysis of the present study also demonstrated a significant difference in delayed enhancement between the two diseases: lesion contrast at DP was less than 1.0 (i.e., $SI_{\text{mass}} > SI_{\text{pancreas}}$) in 91.7% of AIP but was 1.0 or higher (i.e., $SI_{\text{mass}} \leq SI_{\text{pancreas}}$) in 80.6% of PDA. The sensitivity of $\text{Contrast}_{\text{AP}}$ (87.5%) for PDA (cutoff > 1.41) was significantly higher than those of all key imaging features (40.3–68.1%), except for the discrete mass, while maintaining high specificity (94.4%).

Despite the excellent diagnostic performance of $\text{Contrast}_{\text{AP}}$, such quantitative analysis may be difficult to apply in actual clinical practice, which is mainly dependent on the intuitive decision by the readers based on qualitative analysis. Therefore, appropriate qualitative assessment should be supported to enhance the clinical utility of the lesion contrast-related MRI data. Two qualitative factors used to represent $\text{Contrast}_{\text{AP}}$ of quantitative analysis in this study were visually assessed “best phase showing the largest SI difference between the mass and the normal pancreas” and “change of the lesion contrast from UP to AP.” The results of the qualitative analysis were mostly consistent with those of the quantitative analysis. Particularly noteworthy is the change of lesion contrast from UP to AP: the contrast between lesion and the “normal” pancreas decreased in the majority of AIP,

Table 5 Comparison of sensitivity and specificity for the diagnosis of AIP and PDA between Contrast_{AP} and key imaging features

| | Sensitivity (%) | <i>p</i> value* | Specificity (%) | <i>p</i> value* |
|--|-----------------|-----------------|-----------------|-----------------|
| AIP | | | | |
| Contrast _{AP} ≤ 1.41 [#] | 94.4 | | 87.5 | |
| Speckled appearance | 88.9 | 0.688 | 48.6 | < 0.001 |
| Delayed homogeneous enhancement | 80.6 | 0.180 | 94.4 | 0.180 |
| Halo sign | 38.9 | < 0.001 | 100 | 0.004 |
| MPD tapered narrowing | 86.1 | 0.453 | 72.2 | 0.035 |
| Duct penetrating sign | 38.9 | < 0.001 | 95.8 | 0.146 |
| PDA | | | | |
| Contrast _{AP} > 1.41 [#] | 87.5 | | 94.4 | |
| Discrete mass on AP/PP/DP | 95.8 | 0.031 | 72.2 | 0.008 |
| Target enhancement | 68.1 | 0.004 | 94.4 | 1.000 |
| MPD abrupt narrowing | 63.9 | 0.003 | 91.7 | 1.000 |
| MPD marked dilatation | 40.3 | < 0.001 | 94.4 | 1.000 |
| Upstream pancreatic atrophy | 51.4 | < 0.001 | 88.9 | 0.688 |

Abbreviations: MPD, main pancreatic duct; AP, arterial phase; PP, portal phase; DP, delayed phase

[#]Optimal cutoff point calculated by ROC analysis

*Compared with Contrast_{AP}

whereas it mostly increased in PDA. The sensitivity and specificity of “decrease in the visually assessed lesion contrast from UP to AP” for AIP were 72.2% and 88.9%, respectively. The sensitivity and specificity of “increase in the visually assessed lesion contrast from UP to AP” for PDA were 78.8% and 100%, respectively. In other words, between UP and AP, the lesion contrast seldom decreased in PDA, and it increased in none of AIP. Consequently, these findings may be worthy of radiologists’ attention as another key imaging feature to distinguish focal-type AIP from PDA, which can be easily applied in today’s reading environment where the readers can easily compare the images on UP and AP side by side.

Our results regarding the “discrete mass” appear to support the quantitative and qualitative analysis results of the lesion contrast. The frequency of discrete mass on AP/PP/DP (27.8%) was much lower than that on UP (66.7%) in AIP; this may indicate that it became difficult to distinguish the lesion boundary from the surrounding normal parenchyma throughout the contrast-enhanced images as the lesion enhancement starting from AP was strong to some degree. In contrast, PDA had a higher frequency of discrete mass on AP/PP/DP (95.8%) than on UP (83.3%); this result may imply that the lesion boundary was more clearly defined on contrast-enhanced images because the lesion enhancement degree was relatively weaker than the normal parenchyma, especially at AP. Several studies have quantitatively analyzed contrast enhancement using CT in patients with focal-type AIP and PDA, although they did not assess the lesion contrast [9, 16, 18]. These studies also demonstrated that the degree of contrast enhancement at the arterial or pancreatic phase was greater in AIP than in PDA, which may support our conjecture mentioned above.

The appreciable differences in the lesion contrast at AP between focal-type AIP and PDA may be explained in relation

to the following pathological differences of the two diseases as suggested in previous studies [13, 17]. In PDA, there is almost no normal pancreatic tissue remaining inside the mass as the pancreatic parenchyma is almost completely replaced by tumor tissue due to carcinogenesis; moreover, tumor-related fibrosis, i.e., desmoplasia, is mostly profound. In AIP, the pancreatic parenchyma is not totally replaced by the fibrotic mass despite massive lymphoplasmacytic infiltration. Furthermore, acinar cells inside the mass are usually preserved, the lesion distribution is frequently patchy, and interstitial fibrosis is mild [13, 17, 24, 25].

Our study has a few limitations. First, there was a discrepancy in the study period between the two patient groups, i.e., 10 years for the AIP group vs. 3 years for the PDA group, which may have caused variations in the quality of MRI examinations for the AIP group. However, the longer study period for AIP patients was inevitable owing to the rarity of this disease. Second, there may be some intra- and inter-individual variations in the measured SI because the SI in MRI is not standardized, unlike Hounsfield unit in CT, and this could have slightly affected our study results.

In conclusion, the lesion contrast at AP was significantly lower in focal-type AIP than in PDA. Quantitative analysis of the lesion contrast using CE-MRI, particularly at AP, was helpful to differentiate focal-type AIP from PDA. The diagnostic performance of Contrast_{AP} using optimal cutoff point of 1.41 was excellent and mostly comparable to or higher than those of the key imaging features. Therefore, utilization of the Contrast_{AP} in addition to the key imaging features for differentiating between the two diseases may improve the diagnostic accuracy and help establish the prompt and appropriate treatment.

Funding The authors state that this work has not received any funding.

Compliance with ethical standards

Guarantor The scientific guarantor of this publication is Jin Hee Kim.

Conflict of interest The authors of this manuscript declare no relationships with any companies, whose products or services may be related to the subject matter of the article.

Statistics and biometry No complex statistical methods were necessary for this paper.

Informed consent Written informed consent was waived by the Institutional Review Board.

Ethical approval Institutional Review Board approval was obtained.

Methodology

- retrospective
- observational
- performed at one institution

References

1. Finkelberg DL, Sahani D, Deshpande V, Brugge WR (2006) Autoimmune pancreatitis. *N Engl J Med* 355:2670–2676
2. Chari ST, Takahashi N, Levy MJ et al (2009) A diagnostic strategy to distinguish autoimmune pancreatitis from pancreatic cancer. *Clin Gastroenterol Hepatol* 7:1097–1103
3. Kamisawa T, Imai M, Yui Chen P et al (2008) Strategy for differentiating autoimmune pancreatitis from pancreatic cancer. *Pancreas* 37:e62–e67
4. Kim JH, Kim MH, Byun JH et al (2012) Diagnostic strategy for differentiating autoimmune pancreatitis from pancreatic cancer: is an endoscopic retrograde pancreatography essential. *Pancreas* 41: 639–647
5. Kamisawa T, Egawa N, Nakajima H, Tsuruta K, Okamoto A, Kamata N (2003) Clinical difficulties in the differentiation of autoimmune pancreatitis and pancreatic carcinoma. *Am J Gastroenterol* 98:2694–2699
6. Lee S, Kim JH, Kim SY et al (2018) Comparison of diagnostic performance between CT and MRI in differentiating non-diffuse-type autoimmune pancreatitis from pancreatic ductal adenocarcinoma. *Eur Radiol* 28:5267–5274
7. Manfredi R, Frulloni L, Mantovani W, Bonatti M, Graziani R, Mucelli RP (2011) Autoimmune pancreatitis: pancreatic and extrapancreatic MR imaging-MR cholangiopancreatography findings at diagnosis, after steroid therapy, and at recurrence. *Radiology* 260:428–436
8. Rehnitz C, Klauss M, Singer R et al (2011) Morphologic patterns of autoimmune pancreatitis in CT and MRI. *Pancreatol* 11:240–251
9. Takahashi N, Fletcher JG, Hough DM et al (2009) Autoimmune pancreatitis: differentiation from pancreatic carcinoma and normal pancreas on the basis of enhancement characteristics at dual-phase CT. *AJR Am J Roentgenol* 193:479–484
10. Wakabayashi T, Kawaura Y, Satomura Y et al (2003) Clinical and imaging features of autoimmune pancreatitis with focal pancreatic swelling or mass formation: comparison with so-called tumor-forming pancreatitis and pancreatic carcinoma. *Am J Gastroenterol* 98:2679–2687
11. Choi SY, Kim SH, Kang TW, Song KD, Park HJ, Choi YH (2016) Differentiating mass-forming autoimmune pancreatitis from pancreatic ductal adenocarcinoma on the basis of contrast-enhanced MRI and DWI findings. *AJR Am J Roentgenol* 206:291–300
12. Hur BY, Lee JM, Lee JE et al (2012) Magnetic resonance imaging findings of the mass-forming type of autoimmune pancreatitis: comparison with pancreatic adenocarcinoma. *J Magn Reson Imaging* 36:188–197
13. Kim M, Jang KM, Kim JH et al (2017) Differentiation of mass-forming focal pancreatitis from pancreatic ductal adenocarcinoma: value of characterizing dynamic enhancement patterns on contrast-enhanced MR images by adding signal intensity color mapping. *Eur Radiol* 27:1722–1732
14. Negrelli R, Manfredi R, Pedrinolla B et al (2015) Pancreatic duct abnormalities in focal autoimmune pancreatitis: MR/MRCP imaging findings. *Eur Radiol* 25:359–367
15. Furuhashi N, Suzuki K, Sakurai Y, Ikeda M, Kawai Y, Naganawa S (2015) Differentiation of focal-type autoimmune pancreatitis from pancreatic carcinoma: assessment by multiphase contrast-enhanced CT. *Eur Radiol* 25:1366–1374
16. Muhi A, Ichikawa T, Motosugi U et al (2012) Mass-forming autoimmune pancreatitis and pancreatic carcinoma: differential diagnosis on the basis of computed tomography and magnetic resonance cholangiopancreatography, and diffusion-weighted imaging findings. *J Magn Reson Imaging* 35:827–836
17. Sugiyama Y, Fujinaga Y, Kadoya M et al (2012) Characteristic magnetic resonance features of focal autoimmune pancreatitis useful for differentiation from pancreatic cancer. *Jpn J Radiol* 30:296–309
18. Sun GF, Zuo CJ, Shao CW, Wang JH, Zhang J (2013) Focal autoimmune pancreatitis: radiological characteristics help to distinguish from pancreatic cancer. *World J Gastroenterol* 19:3634–3641
19. Otsuki M, Chung JB, Okazaki K et al (2008) Asian diagnostic criteria for autoimmune pancreatitis: consensus of the Japan-Korea Symposium on Autoimmune Pancreatitis. *J Gastroenterol* 43:403–408
20. Chari ST, Smyrk TC, Levy MJ et al (2006) Diagnosis of autoimmune pancreatitis: the Mayo Clinic experience. *Clin Gastroenterol Hepatol* 4:1010–1016 quiz 1934
21. Shimosegawa T, Chari ST, Frulloni L et al (2011) International consensus diagnostic criteria for autoimmune pancreatitis: guidelines of the International Association of Pancreatology. *Pancreas* 40:352–358
22. Carbognin G, Girardi V, Biasutti C et al (2009) Autoimmune pancreatitis: imaging findings on contrast-enhanced MR, MRCP and dynamic secretin-enhanced MRCP. *Radiol Med* 114:1214–1231
23. Chang WI, Kim BJ, Lee JK et al (2009) The clinical and radiological characteristics of focal mass-forming autoimmune pancreatitis comparison with chronic pancreatitis and pancreatic cancer. *Pancreas* 38:401–408
24. Kim HJ, Kim YK, Jeong WK, Lee WJ, Choi D (2015) Pancreatic duct "icicle sign" on MRI for distinguishing autoimmune pancreatitis from pancreatic ductal adenocarcinoma in the proximal pancreas. *Eur Radiol* 25:1551–1560
25. Chandan VS, Iacobuzio-Donahue C, Abraham SC (2008) Patchy distribution of pathologic abnormalities in autoimmune pancreatitis: implications for preoperative diagnosis. *Am J Surg Pathol* 32: 1762–1769

Publisher's note Springer Nature remains neutral with regard to jurisdictional claims in published maps and institutional affiliations.